Free Radical Research, July 2006; 40(7): 731–739

informa
healthcare

A spectroscopic study of some of the peptidyl radicals formed following hydroxyl radical attack on β-amyloid and α-synuclein

BRIAN J. TABNER[1,2], STUART TURNBULL[2], JENNY E. KING[2], FIONA E. BENSON[2], OMAR M.A. EL-AGNAF[2,3] & DAVID ALLSOP[2]

[1]*Magnetic Resonance Laboratory, Department of Biological Sciences, Lancaster University, Lancaster LA1 4YQ, UK,* [2]*Biomedical Sciences Unit, Department of Biological Sciences, Lancaster University, Lancaster LA1 4YQ, UK, and* [3]*Department of Biochemistry, Faculty of Medicine and Health Science, United Arab Emirates University, Abu Dhabi, United Arab Emirates*

Accepted by Professor M. Davies

(Received 15 November 2005; in revised form 26 January 2006)

Abstract

There is clear evidence implicating oxidative stress in the pathology of many neurodegenerative diseases. Reactive oxygen species (ROS) are the primary mediators of oxidative stress, and hydrogen peroxide, a key ROS, is generated during aggregation of the amyloid proteins associated with some of these diseases. Hydrogen peroxide is catalytically converted to the aggressive hydroxyl radical in the presence of Fe(II) and Cu(I), which renders amyloidogenic proteins such as β-amyloid and α-synuclein (implicated in Alzheimer's disease (AD) and Parkinson's disease (PD), respectively) vulnerable to self-inflicted hydroxyl radical attack. Here, we report some of the peptide-derived radicals, detected by electron spin resonance spectroscopy employing sodium 3,5-dibromo-4-nitrosobenzenesulfonate as a spin-trap, following hydroxyl radical attack on Aβ(1–40), α-synuclein and some other related peptides. Significantly, we found that sufficient hydrogen peroxide was self-generated during the early stages of aggregation of Aβ(1–40) to produce detectable peptidyl radicals, on addition of Fe(II). Our results support the hypothesis that oxidative damage to Aβ (and surrounding molecules) in the brain in AD could be due, at least in part, to the self-generation of ROS. A similar mechanism could operate in PD and some other "protein conformational" disorders.

Keywords: *Alzheimer's disease, Parkinson's disease, electron spin resonance, reactive oxygen species, hydroxyl radical, hydrogen peroxide*

Introduction

Alzheimer's disease (AD) is characterised histopathologically by the presence of numerous senile plaques and neurofibrillary tangles in affected regions of the brain. The senile plaques contain extracellular deposits of amyloid fibrils that are composed of a 39–43 amino acid peptide termed "Aβ". Synthetic Aβ peptides (e.g. Aβ(1–40) and Aβ(1–42), which are the most prominent species found in the brain), can aggregate *in vitro* to form fibrils. Upon aggregation, these peptides become toxic to cells. There is increasing evidence that early "soluble oligomers" or "protofibrils" are responsible for this toxicity rather than "mature" amyloid fibrils [1–4], although there is currently no clear consensus regarding the molecular mechanisms involved. Similarly it is now believed that α-synuclein oligomers may also be neurotoxic and play an important role in the pathogenesis of Parkinson's disease (PD) and related disorders [5].

The concept that oxidative stress makes a major contribution to the pathology of several neurodegenerative diseases is receiving mounting support. There is

Correspondence: D. Allsop, Department of Biological Sciences, Lancaster University, Lancaster LA1 4YQ, UK. Tel: 44 1524 592122. Fax: 44 1524 593192. E-mail: d.allsop@lancaster.ac.uk

ISSN 1071-5762 print/ISSN 1029-2470 online © 2006 Informa UK Ltd
DOI: 10.1080/10715760600632545

also evidence indicating that oxidative damage to the brain is one of the earliest pathological events in AD [6–8]. Oxidative stress has been attributed to an imbalance between the production of reactive oxygen species (ROS) (including superoxide, hydrogen peroxide and the hydroxyl radical) and their removal by anti-oxidant defences. Such an imbalance could be a key factor in the aetiology and progression of these diseases. Evidence for oxidative stress includes the detection of features such as the elevation of certain transition metal ion levels (including those of redox-active Cu and Fe ions), lipid peroxidation, the presence of oxidation products of RNA and DNA and the introduction of carbonyl groups into proteins [9–14].

There is a distinct possibility that the accumulation of aggregating forms of Aβ in AD could, either directly or indirectly, result in elevated ROS production in the brain. It has been reported that redox-active transition metal ions such as Cu and Fe ions can bind with high affinity to both Aβ(1–40) and Aβ(1–42) and stimulate their aggregation [15–18]. This binding is accompanied by a decrease in the oxidation state of the metal ion [15,16,19,20]. Behl et al. showed that exposure of cells in culture to Aβ(1–40) and Aβ(25–35) increased hydrogen peroxide levels and that Aβ toxicity was blocked by catalase (a hydrogen peroxide degrading enzyme) [21]. This result implied that hydrogen peroxide is involved at some stage in the toxic process. Evidence for the self-generation of hydrogen peroxide by both Aβ(1–40) and Aβ(1–42) was subsequently presented by Bush and co-workers, employing dye-based colorimetric and fluorometric assays [15–16]. We have confirmed these observations using an alternative technique, based on electron spin resonance (ESR) spectroscopy, and have also established that other Aβ fragments, such as the toxic Aβ(25–35) peptide, share this property [22–25]. We have also demonstrated that some other aggregating proteins (α-synuclein, associated with PD and related disorders [22–25]; ABri, responsible for familial British dementia [26]; and certain toxic fragments of the prion protein, associated with the transmissible spongiform encephalopathies [27–29]), can also generate hydrogen peroxide. Many controls including reverse and scrambled peptides, non-toxic peptides and the β- and γ-synucleins lacked this ability [22–28].

We have shown recently that hydrogen peroxide self-generation occurs as a short "burst" during the early stages of Aβ(1–40) aggregation (when only oligomers are present) and precedes the accumulation of "mature" amyloid fibrils [26]. This source of hydrogen peroxide, and the hydroxyl radicals derived from it in the presence of redox-active transition metal ions, could be responsible for some of the early oxidative damage observed in AD [6–8]. As part of this process, the hydrogen peroxide and hydroxyl radicals could also attack the Aβ peptide itself. The methionine (Met) residue, present in Aβ and α-synuclein, is readily oxidized to methionine sulfoxide (Met(O)) by hydrogen peroxide via two-electron oxidation [30] and Met(O) has been found to be an extensive component of various structural variants of Aβ isolated from AD brain, indicating that oxidation of Met to Met(O) takes place under pathological conditions [31,32]. Here, we have designed a series of experiments to test the hypothesis that *in vivo* oxidative damage to Aβ, and possibly other metal-binding amyloidogenic peptides, could be due, at least in part, to the action of self-generated hydrogen peroxide.

In our initial experiments, Aβ, α-synuclein and some other related test compounds were incubated with an external source of hydrogen peroxide, and then Fe(II) was added to stimulate Fenton's reaction:

$$H_2O_2 + Fe(II) \rightarrow Fe(III) + \cdot OH + {}^{-}OH$$

The hydroxyl radicals so-formed would attack the peptides to give peptidyl radicals. These first experiments were designed to optimise peptidyl radical formation, so that these radicals could be readily detected and characterized. The latter was achieved by ESR spectroscopy, employing sodium 3,5-dibromo-4-nitrosobenzene-sulfonate (DBNBS) as a spin-trap, which was added immediately before the Fe(II). Reagent concentrations were selected so as to maximise the reaction between hydroxyl radicals and the substrate molecule of interest, rather than with DBNBS. Reaction of the hydroxyl radical with this nitroso spin-trap is known to give relatively short-lived adducts, which are not observed in ESR experiments and, consequently, do not interfere. In contrast, however, reaction of the spin-trap with C-centred radicals gives relatively long-lived, detectable, adducts. There is the additional advantage that the C-centred radical is attached directly to the nitroso nitrogen atom of the spin-trap (see Figure 1). This leads to informative hyperfine detail in the ESR spectrum of the DBNBS adduct which originates from the original radical [33].

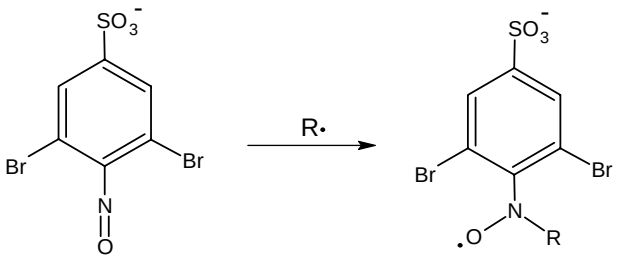

Figure 1. The structure of DBNBS and its spin-adducts.

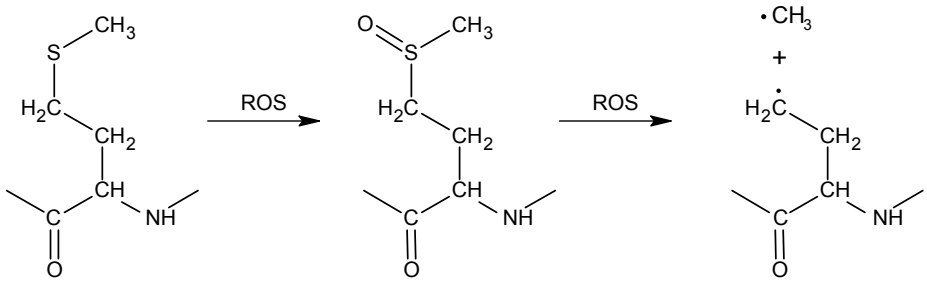

Scheme 1. A schematic reaction pathway showing the formation of the methyl and $\cdot CH_2R$ (1) radicals from the methionine residue in the presence of ROS.

Under these conditions, some Met in the peptides would be converted to Met(O), and our method allows this modified residue to be detected by its reaction with hydroxyl radicals to release C-centred radicals as reaction products [34], see Scheme 1.

Once we had established the hyperfine parameters associated with the DBNBS adducts of the peptidyl radicals under investigation, we then determined whether sufficient hydrogen peroxide was self-generated during the incubation of Aβ(1–40) to induce the formation of detectable peptidyl radicals, upon addition of Fe(II).

We stress that our proposed mechanism for the formation of peptidyl radicals, via the formation of hydrogen peroxide and hydroxyl radicals, is very different to an earlier hypothesis based on spontaneous self-fragmentation of the peptide or protein during incubation (sometimes referred to as the "shrapnel" hypothesis) [35]. The steady-state concentrations of any peptidyl radicals formed by the latter mechanism would be far too low for their detection by our technique.

Materials and methods

Reagents

Reagents were purchased as the highest purity grade available from Aldrich, Bachem, Biosource and Sigma (and were used as supplied) except for the sample of α-synuclein (which was prepared as described below) and one sample of Aβ(1–40) (which was prepared as described) [36]. Sodium 3,5-dibromo-4-nitrosobenzenesulfonate was synthesized as described in the literature [37].

Preparation of α-synuclein

The human α-synuclein gene was amplified from a cDNA clone (IMAGE:4500613) using the polymerse chain reaction (PCR) and subcloned into pET15b to generate plasmid pJEK1. Recombinant human α-synuclein was expressed from the T7 promoter as a $(His)_6$ fusion protein and purified as follows. Plasmid pJEK1 was used to transform the *E. coli* strain FB850, a *rec*A$^-$ derivative of BL21(DE3) pLysS. Bacteria were grown in Luria broth and induced by the addition of 1 mM IPTG, followed by a further 2 h incubation at 37°C. Cells were harvested by centrifugation, resuspended in 25 mM Tris–HCl pH 7.5, 500 mM NaCl, 10% glycerol, 0.02% Triton X-100, 25 mM imidazole, lysed by three cycles of freeze-thaw and insoluble material removed by centrifugation. The soluble protein fraction was loaded onto a 5 ml HiTrap chelating column (Amersham Biosciences) charged with Ni(II) and bound proteins eluted with a linear gradient of imidazole. Peak fractions containing $(His)_6$-α-synuclein were identified by immunoblotting using anti-α-synuclein monoclonal antibodies (Santa Cruz Biotechnology). The $(His)_6$ tag was removed from $(His)_6$-α-synuclein using the thrombin cleavage capture kit (Novagen). The resulting recombinant α-synuclein was dialysed against 20 mM sodium phosphate pH 7.4, 0.5 mM dithiothreitol, 50 mM sodium chloride and loaded onto a MonoQ HR5/5 column (Amersham Biosciences). Bound α-synuclein was eluted with a linear gradient of sodium chloride. Fractions containing monomeric α-synuclein were identified by immunoblotting, pooled and dialysed against 1 × phosphate buffered saline (PBS), pH 7.4. Protein concentration was determined by UV spectroscopy.

Solutions and electron spin resonance spectroscopy

Samples of each molecule (100–250 μM, depending upon solubility) were prepared in PBS, at pH 7.4, in Millipore Milli-Q water in the presence of hydrogen peroxide (70 mM). If required, the solution was incubated in an Eppendorf tube at 37°C, in complete darkness, for periods of up to 96 h and a representative sample (50 μl) withdrawn at the selected time-point. Solutions of diethylenetriaminepentaacetic acid (DETAPAC) (12.5 μl, 125 μM, as metal ion sequestrant), DBNBS (12.5 μl, 30 mM, as spin-trap) and Fe(II) sulfate (12.5 μl, 50 μM) were added and the resulting solution was transferred to an ESR sample tube immediately after mixing. The same procedure

was adopted in some of our experiments involving of Aβ(1–40) (100 μM) except that no additional hydrogen peroxide was added at the beginning of the incubation.

Samples of Met(O) (in PBS solution) were examined, without incubation, by a different procedure in which solutions of DETAPAC, DBNBS, H_2O_2 (12.5 μl 1 mM) and, finally, Fe(II) sulfate were added, mixed and then immediately transferred to an ESR sample tube. No spectra were observed in "control" experiments undertaken in the presence of the appropriate molecule but in the absence of either DBNBS, Fe(II) or H_2O_2. Except in the case of Met(O) no ESR spectra were observed before incubation of the molecule of interest.

Full details of the experimental conditions employed to record ESR spectra have been reported elsewhere [24,28]. Hyperfine splitting constants were measured by spectral simulation using WinSim public software [38]; those of the major spectral components are considered accurate to ± 0.01 mT.

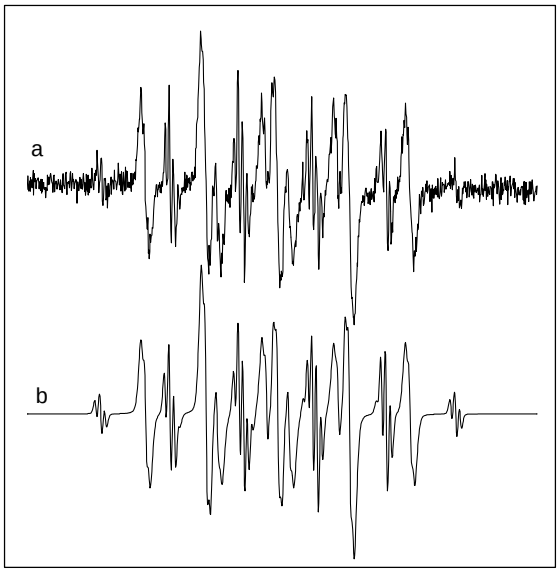

Figure 2. (a) The ESR spectrum (total scan width = 7.5 mT), recorded at room temperature, obtained after addition of DETAPAC, DBNBS, hydrogen peroxide and, finally Fe(II), to an aqueous solution of Met(O) in PBS. (b) A computer simulation of (a), the $\cdot CH_2R$ (1) adduct (80%, a_N 1.41, a_{2Hm} 0.07 and a_{2H} 1.19 mT) and the methyl radical adduct (20%, a_N 1.45, a_{2Hm} 0.08 and a_{3H} 1.34 mT).

Results

ESR investigations of the radicals formed following hydroxyl radical reaction with Met(O), Met and Met–Met–Met

We first examined several model compounds (Met(O), Met and Met–Met–Met) in order to establish the nature of their reaction with ROS and establish the hyperfine parameters associated with the DBNBS adducts of radicals derived from the Met(O) residue (see Scheme 1) under our experimental conditions.

The addition of Fe(II) to a PBS solution of Met(O), DETAPAC, DBNBS and hydrogen peroxide immediately gave an ESR spectrum which was the composite of two DBNBS adducts (see Figure 2(a)). One of these was readily identified as that of the methyl radical (a_N 1.45, a_{2Hm} 0.08 and a_{3H} 1.34 mT) [37], whilst the other was characterized by hyperfine splitting from two equivalent protons (a_N 1.41 a_{2Hm} 0.07 and a_{2H} 1.19 mT). This $\cdot CH_2R$ adduct clearly arises from a radical formed following the alternative homolytic cleavage of the carbon–sulfur bond (see Scheme 1). The spectrum simulation is shown in Figure 2(b).

In most of the remaining experiments reported in this paper the various substrates were incubated in PBS solution at 37°C in the presence of hydrogen peroxide. Solutions of DETAPAC, DBNBS and, finally, Fe(II) (none of which were present during incubation) were added, at the required time-point, to release hydroxyl radicals from the hydrogen peroxide (via the Fenton reaction).

In these experiments spectra were readily observed after a short incubation period. In the case of Met a spectrum was recorded after 30 min incubation with its intensity decreasing slightly after longer incubation periods (of (say) up to 70 h). These spectra were virtually identical with that shown in Figure 2(a) and were readily identified as a mixture of the methyl and $\cdot CH_2R$ radical adducts. Virtually the same spectra, consisting of a mixture of the same two adducts, were also observed upon the incubation of the simple tri-peptide Met–Met–Met for *ca.* 1 h or longer periods (see Scheme 1).

ESR investigations of the radicals formed following hydroxyl radical reaction with Aβ(25–35), Aβ(1–40) and Aβ(1–40)Met35Nle

In all of the spectra described below, which were recorded following hydroxyl radical attack on incubated solutions of the peptide and protein molecules, a second DBNBS adduct of a $\cdot CH_2R$ radical was observed. It was characterised by a smaller a_{2H} hyperfine splitting constant (i.e. a_{2H} *ca.* 0.98 ± 0.02 mT) compared to that observed with Met(O), Met or Met–Met–Met (i.e. a_{2H} *ca.* 1.19 ± 0.01 mT) and hereafter these two adducts are distinguished from one another as adducts of the $\cdot CH_2R$ (2) and $\cdot CH_2R$ (1) radicals respectively.

Hydroxyl radical attack on Aβ(25–35), incubated in the presence of H_2O_2, resulted in a weak spectrum observed after 1 h which was quite different in appearance to those reported above (see Figure 3(a)). The two minor adducts were those observed in the

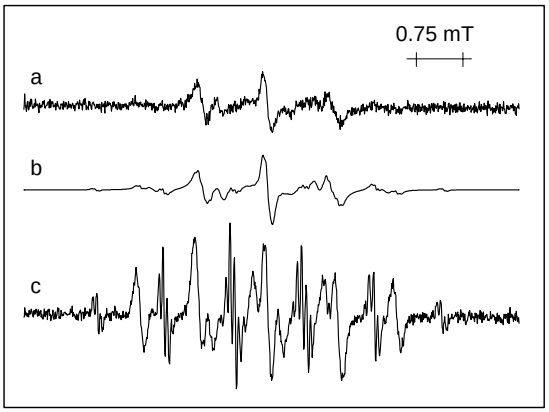

Figure 3. (a) The ESR spectrum, recorded at room temperature, obtained after addition of DETAPAC, DBNBS and, finally Fe(II), to an aqueous solution of Aβ(25–35) in PBS after 1 h incubation in the presence of hydrogen peroxide at 37°C. (b) A computer simulation of (a), the $\cdot CH_2R$ (2) adduct (73%, a_N 1.35, a_{2Hm} 0.07 and a_{2H} 0.98 mT), the $\cdot CR_1R_2R_3$ adduct (12.5%, a_N 1.28 and a_{2Hm} 0.07 mT), the $\cdot CH_2R$ (1) adduct (10%, a_N 1.40, a_{2Hm} 0.07 and a_{2H} 1.18 mT) and the methyl radical adduct (4.5%, a_N 1.48, a_{2Hm} 0.07 and a_{3H} 1.36 mT). (c) As (a) but after 2 h incubation.

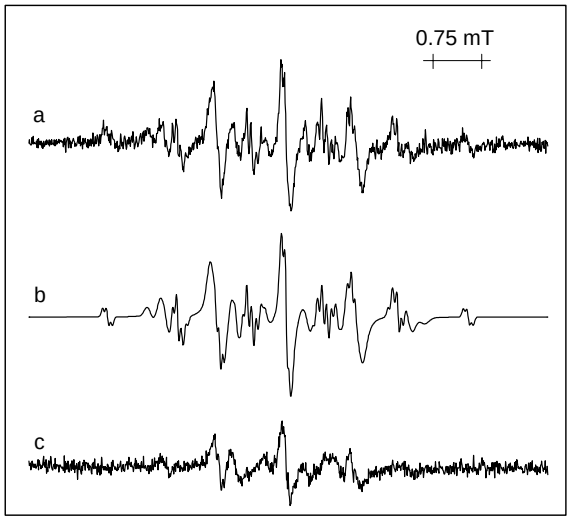

Figure 4. (a) The ESR spectrum, recorded at room temperature, obtained after addition of DETAPAC, DBNBS and, finally Fe(II), to an aqueous solution of Aβ(1–40) in PBS after 6 h incubation in the presence of hydrogen peroxide at 37°C. (b) A computer simulation of (a), the $\cdot CH_2R$ (2) adduct (73%, a_N 1.36, a_{2Hm} 0.07 and a_{2H} 0.97 mT), the methyl radical adduct (13%, a_N 1.44, a_{2Hm} 0.07 and a_{3H} 1.35 mT), the $\cdot CH_2R$ (1) adduct (7.5%, a_N 1.40, a_{2Hm} 0.06 and a_{2H} 1.20 mT) and the $\cdot CR_1R_2R_3$ adduct (6.5%, a_N 1.27 and a_{2Hm} 0.07 mT). (c) The ESR spectrum, recorded at room temperature, obtained after addition of DETAPAC, DBNBS and, finally Fe(II), to an aqueous Aβ(1–40)Met35Nle in PBS after 6 h incubation in the presence of hydrogen peroxide at 37°C.

experiments involving Met(O), Met and Met–Met–Met (i.e. the adducts of the methyl and $\cdot CH_2R$ (1) radicals). However, the two major contributions arose from two new adducts which were again readily identified. One was characterized by hyperfine splitting arising from interaction with two equivalent protons but this time with a_{2H} *ca.* 0.98 mT (i.e. the $\cdot CH_2R$ (2) radical adduct). The second had hyperfine parameters characteristic of a tertiary C-centred radical adduct, $\cdot CR_1R_2R_3$. The computer simulation is shown in Figure 3 (b).

After longer incubation periods (i.e. after *ca.* 2 h or more) the spectra became different in appearance (compare Figure 3(a),(c)) and were very similar to those observed during the experiments involving Met(O), Met and Met–Met–Met consisting of the methyl and $\cdot CH_2R$ (1) radical adducts. There was no significant contribution from the two adducts dominating Figure 3(a) showing that the nature of the radicals present changed as incubation proceeded.

Incubation of Aβ(1–40), in the presence of H_2O_2, resulted in a complex spectrum (upon the addition of the Fe(II) solution) which was observed between 1 and 24 h. The spectrum consisted of the same four components as those observed during the early stages of Aβ(25–35) incubation but present in different relative proportions (see Figure 4(a)). Additional low intensity hyperfine lines were observed in some of these spectra but their poor intensity prevented the accurate determination of any hyperfine parameters.

The ESR spectra recorded during the incubation of Aβ(1–40)Met35Nle (Figure 4(c)), containing no Met residue, were also examined. They could be simulated in terms of just two adducts (those of the $\cdot CH_2R$ (2) and $\cdot CR_1R_2R_3$ radicals) which were present in approximately the same relative proportions as one another.

ESR investigations of the radicals formed following hydroxyl radical reaction with α-synuclein and its non-Aβ component (NAC) fragment

Four identifiable adducts were observed following the incubation of α-synuclein for periods of between 1 and 24 h in the presence of H_2O_2 with the addition of Fe(II) at the required time-point (Figure 5(a)). These adducts had virtually the same hyperfine parameters as those observed during the incubation of Aβ(1–40) but were present in different proportions. The major component was the DBNBS adduct of the $\cdot CH_2R$ (2) radical with minor proportions arising from the other adducts including those derived from Met(O) [see Figure 5(b) for the spectrum simulation]. Again, some additional low intensity hyperfine lines were noticeable in most of these spectra but their intensity was insufficient to allow the accurate determination of any hyperfine parameters associated with them.

A similar study was also undertaken of the non-Aβ component (NAC) of the α-synuclein protein. NAC corresponds to residues 61–95 of the latter and interested us because, like Aβ(1–40)Met35Nle, it also contains no Met residue. The simulation of the (weak)

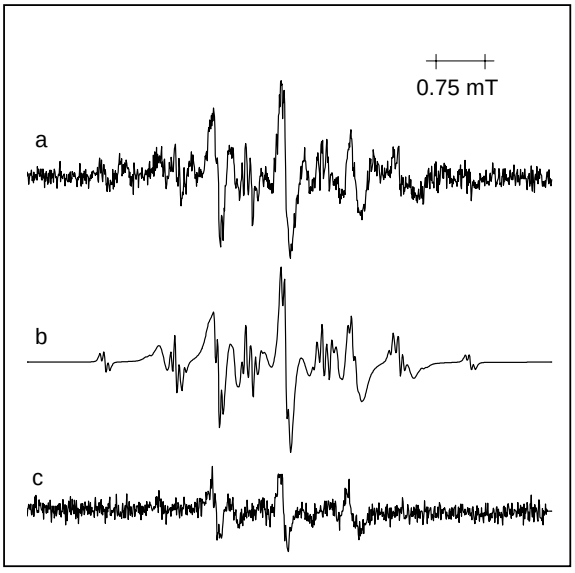

Figure 5. (a) The ESR spectrum, recorded at room temperature, obtained after addition of DETAPAC, DBNBS and, finally Fe(II), to an aqueous α-synuclein in PBS after 1 h incubation in the presence of hydrogen peroxide at 37°C. (b) A computer simulation of (a), the $\cdot CH_2R$ (2) adduct (76%, a_N 1.35, a_{2Hm} 0.07 and a_{2H} 0.98 mT), the methyl radical adduct (14%, a_N 1.46, a_{2Hm} 0.07 and a_{3H} 1.35 mT), the $\cdot CR_1R_2R_3$ adduct (6.5%, a_N 1.27 and a_{2Hm} 0.07 mT) and the $\cdot CH_2R$ (1) adduct (3.5%, a_N 1.40, a_{2Hm} 0.07 and a_{2H} 1.19 mT). (c) The ESR spectrum, recorded at room temperature, obtained after addition of DETAPAC, DBNBS and, finally Fe(II), to a solution of NAC in PBS after 6 h incubation in the presence of hydrogen peroxide at 37°C.

spectra obtained upon hydroxyl radical attack (Figure 5(c)) required the DBNBS adducts of the $\cdot CH_2R$ (2) and $\cdot CR_1R_2R_3$ radicals only.

*ESR investigations of the radicals formed following addition of Fe(II) to A**β**(1–40) incubated in the absence of any added hydrogen peroxide*

Finally, experiments were undertaken in which Aβ(1–40) was incubated (at 100 μM) in the absence of the deliberate addition of hydrogen peroxide at the commencement of the experiment. Aβ(1–40) was selected for these experiments because our batch of peptide conveniently self-generated hydrogen peroxide, as a short burst, after as little as 1 h incubation [26], whereas our sample of recombinant α-synuclein took several days. In addition, peptide aggregation (at this same concentration) had been monitored for this batch of Aβ(1–40) by both the ELISA and thioflavin T methods, as well as by atomic force microscopy (AFM), with the progress of hydrogen peroxide evolution being followed by ESR spectroscopy [26]. The addition of Fe(II) to a representative sample of the incubating Aβ(1–40) solution, at the required time-point, released hydroxyl radicals from any hydrogen peroxide generated at that time. No DBNBS adducts were observed in the ESR

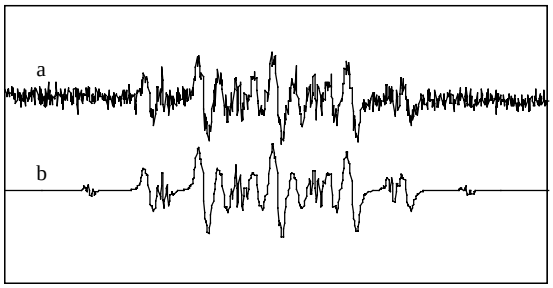

Figure 6. (a) The ESR spectrum (total scan width = 7.5 mT), recorded at room temperature, after addition of DETAPAC, DBNBS and, finally Fe(II), to Aβ(1–40) in PBS after 1 h incubation. (b) A computer simulation of (a), the $\cdot CH_2R$ (2) adduct (84%, a_N 1.37, a_{2Hm} 0.07 and a_{2H} 1.00 mT) and the methyl radical adduct (16%, a_N 1.45, a_{2Hm} 0.08 and a_{3H} 1.35 mT).

spectrum of samples withdrawn at the commencement of incubation (i.e. $t = 0$). Adducts were observed, however, after approximately 1 h incubation. In this latter case, and in samples examined over the first few hours, significantly different spectra (dominated by the methyl and $\cdot CH_2R$ (1) radical adducts) were observed. These spectra (see Figure 6(a)) were somewhat weaker than those observed in some of our other experiments and slowly declined in intensity such that at longer incubation periods (i.e. say 48 h) no adducts could be detected.

Discussion

It has been established for some considerable time that hydroxyl radicals attack a variety of proteins and peptides, resulting in multiple changes in the target molecules [39]. Our observation that C-centred peptidyl radicals were formed following hydroxyl radical attack on target molecules relevant to AD and PD was, therefore, not unexpected. However, our primary objectives were to establish whether or not our ESR approach could reliably detect these radicals, and whether sufficient hydrogen peroxide would be self-generated during the incubation of Aβ alone to result in the detectable formation of peptidyl radicals, on addition of Fe(II).

Much of our attention has focussed on the Met residue since this is one of the most useful in ESR spin-trapping experiments. Sulfides are readily converted to the corresponding sulfoxides in high yield upon reaction with H_2O_2 at ambient temperature. The latter are known hydroxyl radical scavengers and liberate distinctive C-centred radicals upon reaction with ·OH [40]. Our experiments with model compounds were, therefore, designed to establish the hyperfine parameters of the DBNBS adducts of the liberated methyl and the $\cdot CH_2R$ (1) radicals (see the Scheme 1).

In order to follow this first objective, spectra were recorded, following hydroxyl radical attack on the

various target molecules, at various time points of 1 h to extended periods, often up to 96 h. In these experiments the hydroxyl radical was formed when required by reaction with the hydrogen peroxide added at the commencement of each experiment by addition of a solution of Fe(II) ions. In all cases the main two new DBNBS adducts observed were those of the $\cdot CH_2R$ (2) and $\cdot CR_1R_2R_3$ peptidyl radicals derived from the target molecules themselves. These latter two adducts were more difficult to observe in the case of Aβ(25–35) after incubation periods of 2 h or longer. We noted the two adducts derived from the Met(O) residue, in experiments involving Aβ(1–40), Aβ(25–35) and α-synuclein, after as little as 1 h incubation indicating the rapid oxidation of the Met residue. We also noted additional low intensity hyperfine lines in our experiments involving Aβ(1–40) and α-synuclein. Although their intensity prevented any accurate determination of the residues attacked, the magnitude of the hyperfine splitting constants suggests that these lines were associated with the DBNBS adducts of radicals derived from residues with an aromatic component.

In our experiments involving Aβ(1–40)Met35Nle and NAC the two adducts of the radicals derived from the Met(O) residue were absent and these peptides acted as "controls" providing useful information on the adducts detected from residues other than Met and Met(O). The result of our experiments involving NAC particularly interested us because the Met residue appears to play an important role in the aggregation and neurotoxicity of peptides relevant to AD [41,42]. However, the presence of this residue cannot be critical in all peptides as NAC forms aggregates, is highly toxic, and also liberates hydrogen peroxide, but lacks Met [22]. Clearly more than one residue can play an important role in promoting these properties [23].

Our final experiments, in which no hydrogen peroxide was present at the beginning of the experiment, show that sufficient hydrogen peroxide was self-generated after as little as 1 h incubation of Aβ(1–40) to enable the release of some hydroxyl radicals upon the addition of the Fe(II) solution. These radicals attacked the peptide to form the $\cdot CH_2R$ (1) radical and the methyl radical DBNBS adducts (see Scheme 1) indicating that some of the Met residue must have been oxidised to Met(O), even at this early stage. Under these experimental conditions, small Aβ oligomers would be expected to be present, but not mature amyloid fibrils [26]. The lack of any adducts in spectra recorded after longer incubation periods (of, say, 48–96 h) suggests that insufficient hydrogen peroxide remained in these solutions at this time to allow the significant formation of the hydroxyl radical, upon the addition of Fe(II). This slow decline in hydrogen peroxide levels after an initial formation burst is supported by the findings reported in our earlier publication [26].

Whilst it is possible to clearly identify the radicals derived from the methionine sulfoxide residue it is not possible to state categorically which other residues (including any un-oxidised Met) are actually attacked by the hydroxyl radical *in vitro* to result in the $\cdot CH_2R$ (2) and $\cdot CR_1R_2R_3$ radicals. As with all spin-trapping experiments it is important to bear in mind that the species trapped may not be the most abundant radical species present. Steric factors can be very important and, in addition, the trapping reaction follows competitive kinetics. It is quite possible that radical reactions such as transformation and rearrangement may occur before reaction with DBNBS. Additionally, it is not always possible to categorically identify the DBNBS adducts of either primary or tertiary C-centred radicals due to the similarity of their ESR parameters, although the latter is consistent with a backbone radical. Reaction kinetics suggest that hydroxyl radical attack on the target molecule would be relatively random and that any cross-linking between resulting peptidyl radicals would be non-specific. However, we believe that the exact sites of attack on peptides and proteins relevant to AD and PD are likely to be in the vicinity of redox-active transition metal binding sites, where there is a supply of electrons and the conversion of hydrogen peroxide to hydroxyl radicals is most likely to take place. The very high reactivity of this latter radical ensures attack would take place at these, or closely neighbouring sites, leading to more specific cross-linking than might have been anticipated.

The accumulation of results from these, and other laboratories, suggests a hypothesis for the pathogenesis of AD, PD and related disorders when antioxidant defences prove inadequate. The process appears to be initiated by the binding of certain redox-active transition metal ions to the aggregating protein or peptide involved. Only trace concentrations of metal ions appear to be required. Electron transfer reactions then convert oxygen to hydrogen peroxide and reduce the oxidation state of the metal ions. This self-generation of hydrogen peroxide occurs as a burst very early during the aggregation process [26]. Some of the hydrogen peroxide is converted to aggressive hydroxyl radicals via Fenton chemistry, and our results now show that sufficient ROS can be generated experimentally in this way from Aβ to induce oxidative self-damage to the peptide. This process could partly explain the presence of the Met(O) variant of Aβ in AD brain [31,32]. Moreover, our results also suggest that *in vivo*, in the presence of redox-active metal ions to stimulate Fenton's reaction, Aβ would be potentially capable of inducing oxidative damage not only to itself but also to any other molecules in its immediate vicinity. The hydroxyl radicals formed in this way would attack amino acid residues in proteins to form C-centred peptide-derived radicals. In the case of Aβ and other amyloid fibril-forming proteins, these

C-centred radicals could contribute to cross-linking and, perhaps, to stabilisation of early oligomers, and so, themselves, play a role in initiating and sustaining the early stages of aggregation [43]. *In vivo* these reactions are likely to be supplemented by the generation of ROS form other sources, for example from activated microglial cells, leading to damage of cellular constituents and, ultimately, to widespread oxidative brain damage.

Acknowledgements

This research was supported by a project grant from The Wellcome Trust (grant GR065764AIA).

References

[1] Walsh DM, Hartley DM, Kusumoto Y, Fezoui Y, Condron MM, Lomakin A, Benedek GB, Selkoe DJ, Teplow DB. Amyloid β-protein fibrillogenesis. Structure and biological activity. J Biol Chem 1999;274:25945–25952.

[2] Kayed R, Head E, Thompson JL, McIntire TM, Milton SC, Cotman CW, Glabe CG. Common structure of soluble amyloid oligomers implies common mechanism of pathogenesis. Science 2003;300:486–489.

[3] Stefani M, Dobson CM. Protein aggregation and aggregate toxicity: New insights into protein folding misfolding diseases and biological evolution. J Mol Med 2003;81:678–699.

[4] Chromy BA, Nowak RJ, Lambert MP, Viola KL, Chang L, Velasco PT, Jones BW, Fernandez SJ, Lacor PN, Horowitz P, Finch CE, Krafft GA, Klein WL. Self-assembly of Aβ(1–42) into globular neurotoxins. Biochemistry 2003; 42:12749–12760.

[5] Glaser CB, Yamin G, Uversky VN, Fink AL. Methionine oxidation, α-synuclein and Parkinson's disease. Biochim Biophys Acta 2005;1703:157–169.

[6] Nunomura A, Perry G, Aliev G, Hirai K, Takeda A, Balraj EK, Jones PK, Ghanbari H, Wataya T, Shimohama S, Chiba S, Atwood CS, Petersen RB, Smith MA. Oxidative damage is the earliest event in Alzheimer disease. J Neuropathol Exp Neurol 2001;60:759–767.

[7] Beal MF. Oxidative damage as an early marker of Alzheimer's disease and mild cognitive impairment. Neurobiol Aging 2005;26:585–586.

[8] Keller JN, Schmitt FA, Scheff SW, Ding Q, Chen Q, Butterfield DA, Markesbury WR. Evidence of increased oxidative damage in subjects with mild cognitive impairment. Neurology 2005;64:1152–1156.

[9] Markesbery WR. Oxidative stress hypothesis in Alzheimer's disease. Free Radic Biol Med 1997;23:134–147.

[10] Miranda S, Opazo C, Larrondo LF, Muñoz FJ, Ruiz F, Leighton F, Inestrosa NC. The role of oxidative stress in the toxicity induced by amyloid β-peptide in Alzheimer's disease. Prog Neurobiol 2000;62:633–648.

[11] Sayre LM, Smith MA, Perry G. Chemistry and biochemistry of oxidative stress in neurodegenerative disease. Curr Med Chem 2001;8:721–738.

[12] Butterfield DA, Drake J, Pocernich C, Castegna A. Evidence of oxidative damage in Alzheimer's disease brain: Central role for amyloid β-peptide. Trends Mol Med 2001;7:548–554.

[13] Beal MF. Oxidatively modified proteins in aging and disease. Free Radic Biol Med 2002;32:797–803.

[14] Barnham KJ, Masters CL, Bush AI. Neurodegenerative diseases and oxidative stress. Nat Rev Drug Discov 2004;3:205–214.

[15] Huang XD, Atwood CS, Hartshorn MA, Multhaup G, Goldstein LE, Scarpa RC, Cuajungco MP, Gray DN, Lim J, Moir RD, Tanzi RE, Bush AI. The Aβ peptide of Alzheimer's disease directly produces hydrogen peroxide through metal ion reduction. Biochemistry 1999;38:7609–7616.

[16] Huang XD, Cuajungco MP, Atwood CS, Hartshorn MA, Tyndall JDA, Hanson GR, Stokes KC, Leopold M, Multhaup G, Goldstein LE, Scarpa RC, Saunders AJ, Lim J, Moir RD, Glabe C, Bowden EF, Masters CL, Fairlie DP, Tanzi RE, Bush AI. Cu(II) potentiation of Alzheimer Aβ neurotoxicity—correlation with cell-free hydrogen peroxide production and metal reduction. J Biol Chem 1999;274:37111–37116.

[17] Atwood CS, Scarpa RC, Huang XD, Moir RD, Jones WD, Fairlie DP, Tanzi RE, Bush AI. Characterization of copper interactions with Alzheimer amyloid β peptides: Identification of an attomolar-affinity copper binding site on amyloid β 1–42. J Neurochem 2000;75:1219–1233.

[18] Miura T, Suzuki K, Takeuchi H. Binding of iron(III) to the single tyrosine residue of amyloid β-peptide probed by Raman spectroscopy. J Mol Struct 2001;598:79–84.

[19] Curtain CC, Ali F, Volitakis I, Cherny RA, Norton RS, Beyreuther K, Barrow CJ, Masters CL, Bush AI, Barnham KJ. Alzheimer's disease amyloid-β binds copper and zinc to generate an allosterically ordered membrane-penetrating structure containing superoxide dismutase-like subunits. J Biol Chem 2001;276:20466–20473.

[20] Opazo C, Barría MI, Ruiz FH, Inestrosa NC. Copper reduction by copper binding proteins and its relation to neurodegenerative diseases. BioMetals 2003;16:91–98.

[21] Behl C, Davis JB, Lesley R, Schubert D. Hydrogen peroxide mediates amyloid-β protein toxicity. Cell 1994;77:817–827.

[22] Turnbull S, Tabner BJ, El-Agnaf OMA, Allsop D. α-Synuclein implicated in Parkinson's disease catalyses the formation of hydrogen peroxide *in vitro*. Free Radic Biol Med 2001;30:1163–1170.

[23] Tabner BJ, Turnbull S, El-Agnaf OMA, Moore S, Davies Y, Allsop D. Production of reactive oxygen species from aggregating proteins implicated in Alzheimer's disease, Parkinson's disease and other neurodegenerative diseases. Curr Top Med Chem 2001;1:507–517.

[24] Tabner BJ, Turnbull S, El-Agnaf OMA, Allsop D. Formation of hydrogen peroxide and hydroxyl radicals from Aβ and α-synuclein as a possible mechanism of cell death in Alzheimer's disease and Parkinson's disease. Free Radic Biol Med 2002;32:1076–1083.

[25] Tabner BJ, Turnbull S, El-Agnaf OMA, Allsop D. Direct production of reactive oxygen species from aggregating proteins and peptides implicated in the pathogenesis of neurodegenerative diseases. Curr Med Chem—Immunol Endocr Metab Agents 2003;3:299–308.

[26] Tabner BJ, El-Agnaf OMA, Turnbull S, German MJ, Paleologou KE, Hayashi Y, Cooper LJ, Fullwood NJ, Allsop D. Hydrogen peroxide is generated during the very early stages of aggregation of the amyloid peptides implicated in Alzheimer disease and familial British dementia. J Biol Chem 2005;280:35789–35792.

[27] Turnbull S, Tabner BJ, Brown DR, Allsop D. Copper-dependent generation of hydrogen peroxide from the toxic prion protein fragment PrP106–126. Neurosci Lett 2003;336:159–162.

[28] Turnbull S, Tabner BJ, Brown DR, Allsop D. Generation of hydrogen peroxide from mutant forms of the prion protein fragment PrP121-231. Biochemistry 2003;42:7675–7681.

[29] Turnbull S, Tabner BJ, Brown DR, Allsop D. Quinacrine acts as an antioxidant and reduces the toxicity of the prion peptide PrP106-126. Neuroreport 2003;14:1743–1745.

[30] Schöneich C. Methionine oxidation by reactive oxygen species: Reaction mechanisms and relevance to Alzheimer's disease. Biochim Biophys Acta 2005;1703:111–119.

[31] Naslund J, Schierhorn A, Hellman U, Lannfelt L, Roses AD, Tjernberg LO, Silberring J, Gandy SE, Winblad B, Greengard P, Norstedt C, Terenius L. Relative abundance of Alzheimer Aβ amyloid peptide variants in Alzheimer's disease and normal aging. Proc Natl Acad USA 1994;91:8378–8382.

[32] Dong J, Atwood CS, Anderson VE, Siedlak SL, Smith MA, Perry G, Carey PR. Metal binding and oxidation of amyloid-β within isolated senile plaque cores: Raman microscopic evidence. Biochemistry 2003;42:2768–2773.

[33] Davies MJ, Hawkins CL. EPR spin trapping of protein radicals. Free Radic Biol Med 2004;36:1072–1086.

[34] Nakao LS, Iwai LK, Kalil J, Augusto O. Radical production from free and peptide-bound methionine sulfoxide oxidation by peroxynitrite and hydrogen peroxide/iron(II). FEBS Lett 2003;547:87–91.

[35] Hensley K, Carney JM, Mattson MP, Aksenova M, Harris M, Wu JF, Floyd RA, Butterfield DA. A model for β-amyloid aggregation and neurotoxicity based on free-radical generation by the peptide: Relevance to Alzheimer disease. Proc Natl Acad Sci USA 1994;91:3270–3274.

[36] El-Agnaf OMA, Goodwin H, Sheridan JM, Frears ER, Austen BM. Improved solid phase syntheses of amyloid proteins associated with neurodegenerative diseases. Protein Pept Lett 2000;7:1–8.

[37] Kaur H, Leung KHW, Perkins MJ. A water-soluble nitroso-aromatic spin-trap. J Chem Soc Chem Commun 1981; 142–143.

[38] Duling DR. Simulation of multiple isotropic spin-trap EPR-spectra. J Magn Reson B 1994;104:105–110.

[39] Davies MJ. The oxidative environment and protein damage. Biochim Biophys Acta 2005;1703:93–109.

[40] Lagercrantz C, Forshult S. Trapping of short-lived free radicals as nitroxide radicals detectable by ESR spectroscopy. Radicals formed in reaction between OH-radicals and some sulphoxides and sulphones. Acta Chem Scand 1969;23:811–817.

[41] Schöneich C, Pogocki D, Hug GL, Bobrowski B. Free radical reactions of methionine in peptides: Mechanisms relevant to β-amyloid oxidation and Alzheimer's disease. J Am Chem Soc 2003;125:13700–13713.

[42] Butterfield DA, Bush AI. Alzheimer's amyloid β-peptide (1–42): Involvement of methionine residue 35 in the oxidative stress and neurotoxicity properties of this peptide. Neurobiol Aging 2004;25:563–568.

[43] Ali FE, Leung A, Cherny RA, Mavros C, Barnham KJ, Separovic F, Barrow CJ. Dimerisation of *N*-acetyl-L-tyrosine ethyl ester and Aβ peptides via formation of dityrosine. Free Radic Res 2006;40:1–9.